Chapter 2

Physical Processes Governing Neutrals

2.1 Introduction

Multiple physical processes are responsible for the creation, destruction, and visibility of Io's corona and neutral clouds. In this chapter I discuss many of the physical processes that together create the unique neutral clouds observed at Jupiter. In Section 2.2, I describe the processes of resonant scattering, which allows sodium to be observed, and electron impact excitation, the process which dominates the oxygen and sulfur emission. Next I describe sputtering, the main source of neutral escape from Io's exobase. Section 2.4 describes the two processes which limit the size of the neutral clouds: electron impact ionization and charge exchange. The chapter concludes with a summary of the forces which act on the neutrals between their loss from Io (i.e., their entry into the clouds) and their loss by ionization. The specific application of these physical processes to the neutral clouds will be discussed in Chapter 5 where the neutral cloud model is introduced.

2.2 Emission and Absorption Mechanisms

Knowing which microscopic physical processes are responsible for producing the observed radiation from an astrophysical object is a good first step in understanding the properties of the object. This section describes the processes which allow Iogenic neutrals to be observed both in emission and absorption. The first mechanism, resonant

scattering, applies only to sodium and explains why sodium is the most commonly observed neutral at Io. The second mechanism, electron impact excitation, is the main mechanism responsible for emission by oxygen and sulfur. A small component of the sodium emission is due to electron impact excitation of sodium, but since this is small compared to the emission by resonant scattering, it is not included in this work.

2.2.1 Resonant Scattering: Observing Sodium

The sodium observations discussed in this thesis reveal the presence of sodium either through emission or absorption. The same physical mechanism is responsible in each case: the resonant scattering of light by sodium atoms. As sunlight interacts with sodium atoms, photons are absorbed and almost instantly re-emitted (within $\sim 10^{-8}\,sec$). Since the incident photons all originate from the same direction (the direction of the sun) and are emitted isotropically, an observer looking along the sun-Io line (with Io between the sun and the observer) will see the intensity of sunlight at the resonant wavelengths diminished; i.e., an absorption line. When observing off the direct line-of-sight to the sun, sodium is observed in emission.

The two main advantages of observing resonantly scattered sodium are that the cross sections for the resonant transitions are large resulting in strong spectral features, and that the intensity depends only on the column density of sodium and the intensity of incident sunlight, not on the state of the plasma flowing through it. It is much easier to derive the sodium density in the neutral cloud than the oxygen density since the intensity of oxygen emission is strongly dependent on the the plasma exciting the emission.

The radiative transfer of the sodium D lines ($3s\,^2S_{1/2} \rightarrow\ 3p\,^2P_{1/2}, 3p\,^2P_{3/2}$) is discussed here to show how the observed absorption or emission relates to the column density of sodium. The lines connect to the ground state and are excited by absorption of solar photons. Figure 2.1 shows a schematic of these transitions including the hyperfine

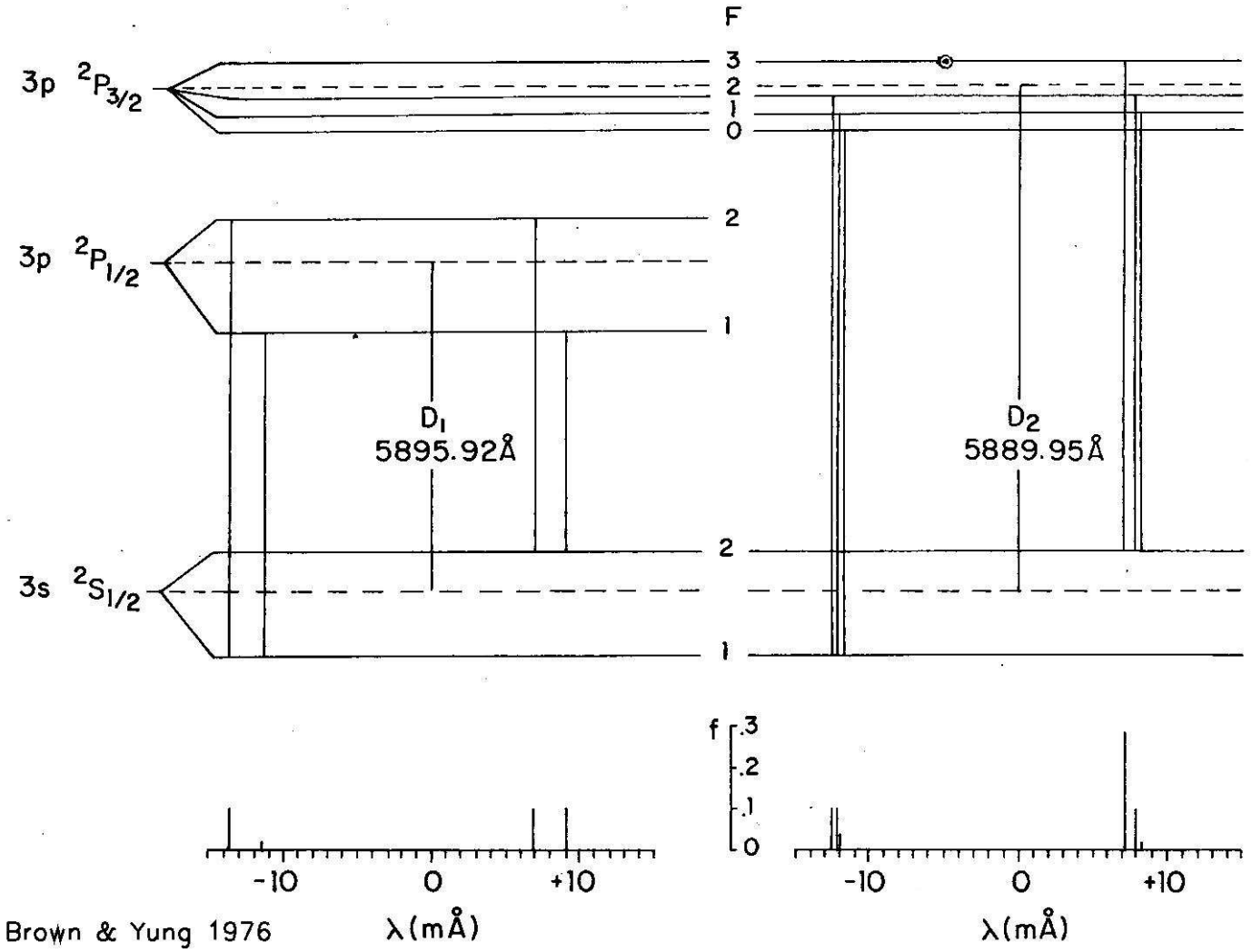

Figure 2.1 From Brown and Yung (1976): Schematic of the sodium D resonance transitions

structure. Hyperfine structure must be included to properly determine the curve of growth (equivalent width vs. column density plot). The following is based on discussions of resonant scattering of sunlight by sodium in Chamberlain (1961) and Brown and Yung (1976).

The fraction of incident sunlight not absorbed by sodium atoms is determined by:

$$T = e^{-\tau} = e^{-\sigma(\lambda)N} \tag{2.1}$$

where $\tau = \sigma(\lambda)N$ is the optical depth through a cloud of sodium atoms with column density N. The wavelength dependent absorption cross section coefficient ($\sigma(\lambda)$) is the sum of the individual Doppler broadened hyperfine line profiles:

$$\sigma = \sum \sigma_i = \sum \sigma_{0i} e^{\frac{(\lambda-\lambda_{0i})^2}{\alpha_i^2}} \tag{2.2}$$

The cross section at the center of hyperfine line i is given by

$$\sigma_{0i} = \left(\frac{\lambda_{0i}^2}{c\sqrt{\pi}\alpha_i}\right)\left(\frac{\pi e^2}{m_{Na}c}\right) f_i \tag{2.3}$$

The Doppler broadening constant α depends on the temperature according to:

$$\alpha_i = \frac{\lambda_{0i}}{c}\sqrt{\frac{2kT}{m_{Na}}} \tag{2.4}$$

The offsets of each hyperfine line from the central wavelengths ($\Delta\lambda$) and their oscillator strengths (f_i) are listed in Table 2.1.

The measured quantity for an absorption line is the equivalent width, defined as

$$W_\lambda = \int_{-\infty}^{\infty}(1-T)d\lambda = \int_{-\infty}^{\infty}(1-e^{-\tau})d\lambda \tag{2.5}$$

and is a function of the sodium column density and temperature. The curves of growth for the D_2 line and the ratio of W_{D_2} to W_{D_1} at several temperatures are shown in Figure 2.2. For optically thin regions ($\tau < 1$) the equivalent width is linear with column density (on the log-log plot) and independent of temperature. When the sodium is optically thick ($\tau \gtrsim 1$), the degeneracy in temperature is lifted and the equivalent width

$D_1\ ^2S_{1/2} \rightarrow ^2P_{1/2}$, $\lambda_{D_1} = 5895.92$ Å, f=0.33		
Hyperfine Transition	$\boldsymbol{\Delta\lambda}$**(mÅ)**	**f**
F=2 → F=1	-13.6	0.102
F=1 → F=1	-11.4	0.020
F=2 → F=2	+6.9	0.102
F=1 → F=2	+9.1	0.102
$D_2\ ^2S_{1/2} \rightarrow ^2P_{3/2}$, $\lambda_{D_2} = 5889.95$ Å, f=0.65		
Hyperfine Transition	$\boldsymbol{\Delta\lambda}$**(mÅ)**	**f**
F=2 → F=1	-12.6	0.102
F=1 → F=1	-12.2	0.102
F=0 → F=1	-12.0	0.041
F=3 → F=2	+7.2	0.287
F=2 → F=2	+7.9	0.102
F=1 → F=2	+8.3	0.020

Table 2.1 Sodium D Line Parameters (from Brown and Yung (1976))

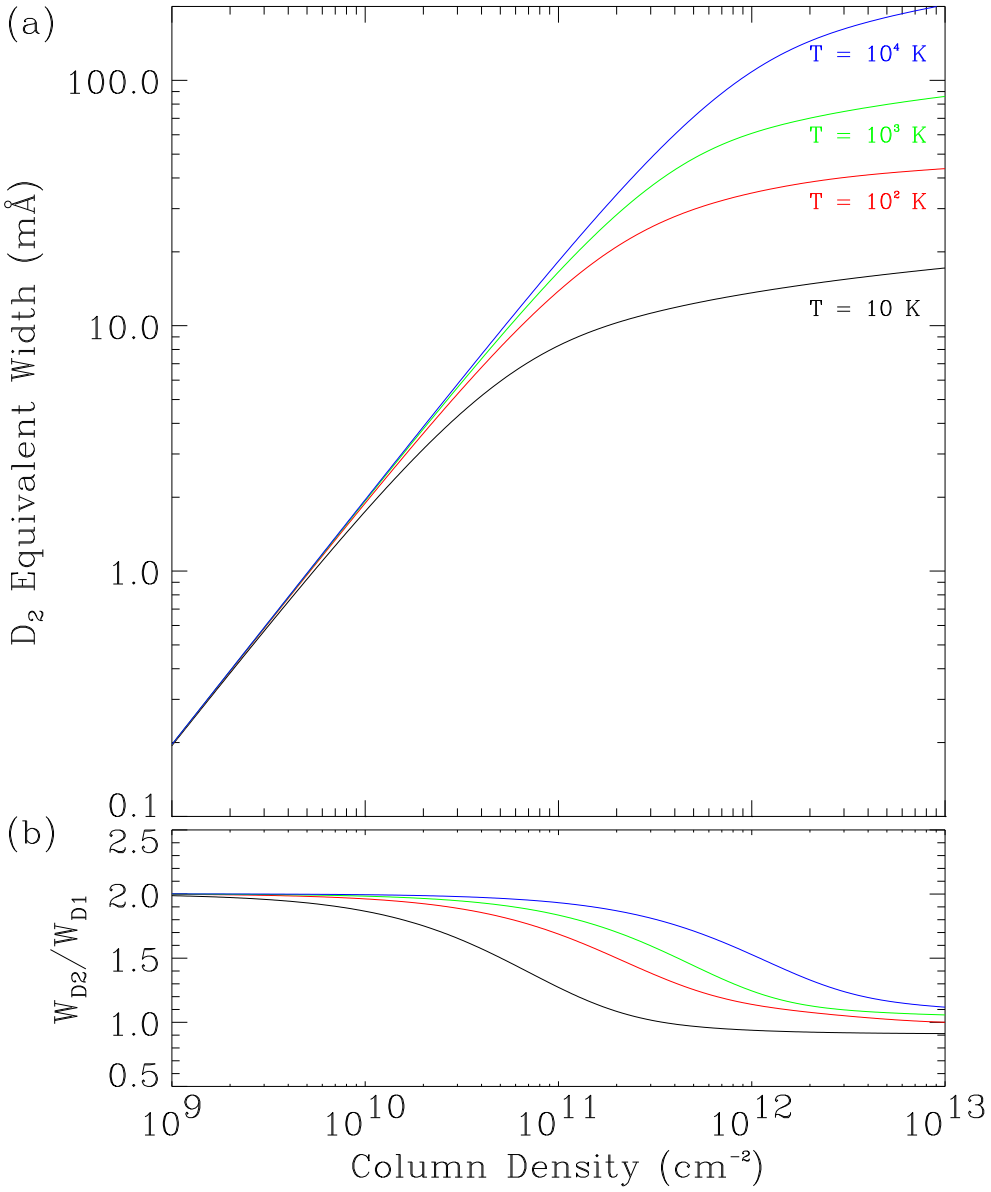

Figure 2.2 (a) Curves of growth for the Na D_2 line at 5890 Å for four temperatures. (b) Ratio of equivalent widths of D_2 and D_1 lines at the four temperatures in (a). Note that, $W_{D_2}/W_{D_1} = 2$ for low column densities and approaches 1 for high column densities.

increases by $\sqrt{\ln(\sigma N)}$. The transition point between the optically thin and optically thick regimes is a function of temperature. Note that in the optically thin regime, the ratio of W_{D2} to W_{D1} reduces to the ratio of the oscillator strengths of the two lines, in this case, $W_{D2}/W_{D1} \rightarrow 2$ (Figure 2.2b). As the column of absorbing sodium increases, the ratio of equivalent widths approaches 1, providing a simple estimate of the optical depth.

When viewing from a geometry other than directly along the sun-Io line, sodium is seen in emission. The absorbed photons are emitted isotropically (the D_2 line is slightly anisotropic (Parkinson 1975), but for these purposes, it is assumed to be isotropic). The observed sodium intensity coupled with knowledge of the intensity of the solar continuum at sodium D wavelengths directly determines the column density.

When the gas is optically thin, the intensity is given by

$$E = gN \tag{2.6}$$

where N is the column density and the g-factor is the rate of photon absorption per neutral atom defined by

$$g = \left[\gamma \cdot \pi F_{\odot}(5900\mathring{A}) \cdot \frac{\lambda^2}{c}\right] \left(\frac{\pi e^2}{m_e c}\right) f \tag{2.7}$$

The term $\left(\gamma \cdot \pi F_{\odot} \frac{\lambda^2}{c}\right)$ is the total number of photons available for absorption in units of photons cm^{-2}, and $\left(\frac{\pi e^2}{m_e c} f\right)$ is the absorption coefficient in $cm^2\ s^{-1}$. The solar continuum flux at the sodium D wavelengths is $\pi F_{\odot}(5900\mathring{A}) = 2.02 \times 10^{12}\, photons \cdot cm^{-2} \cdot \mathring{A}^{-1} \cdot s^{-1}$. The term $\left(\gamma \cdot \pi F_{\odot}(5900\mathring{A})\right)$ is the solar flux at the absorption wavelength in Io's rest frame, where γ is the ratio of the solar intensity at the sodium line Doppler shifted to Io's rest frame to the continuum (see Figure 1.2). If Io's radial velocity relative to the Sun is 0 km s^{-1} then for the two Na D lines, $\gamma_{D2} = 0.05$ and $\gamma_{D1} = 0.06$ (Brown and Yung 1976). At Io's maximum radial velocity of $\pm$ 17.3 km s^{-1} (corresponding to eastern and western elongation), $\gamma_{D2} = 0.6$ and $\gamma_{D1} = 0.7$. Since the emitted intensity

is directly proportional to γ, there is an order of magnitude change in the brightness of the sodium cloud over Io's orbital period simply because of the change in Io's radial velocity relative to the sun.

Converting Equation 2.6 to the unit of choice for line emission measurements, the Rayleigh ($1Ra = 10^6\, photons \cdot cm^{-2} \cdot s^{-1} \cdot (4\pi ster)^{-1}$), yields:

$$\begin{aligned} E_{D_2} &= (3.9 \times 10^{-7} Ra \cdot cm^2)\, \gamma_{D_2}\, N \\ E_{D_1} &= (2.0 \times 10^{-7} Ra \cdot cm^2)\, \gamma_{D_1}\, N \end{aligned} \tag{2.8}$$

For regions where sodium is optically thick, multiple scatterings become important and a more detailed model of the radiative transfer is needed to correctly determine the column density from the brightness. Since sodium is only optically thick in the corona near Io, where the emission can not easily be observed from Earth, it is not necessary to do this modeling here. A method to determine the column density of sodium from optically thick absorption lines is described in chapter 3.

2.2.2 Electron Impact Excitation: Observing oxygen and sulfur

Oxygen and sulfur are not observed through resonant scattering like the trace constituent sodium. Instead, the emission observed for these neutrals is excited by electron impacts. It is more difficult to determine the column density of the emitting region for electron excited emission due to the fact the the emitted intensity depends not only on the number of neutrals present, but also on the properties of the plasma that bathes the neutrals and which varies considerably along the line of sight. The morphology of the emitting region is therefore sensitive to both the distribution of neutrals and changes in the plasma.

The emission intensity is determined by integrating the volume emission rate ρ_k over the line-of-sight. The volume emission rate in units of $cm^{-3}s^{-1}$ is:

$$\rho_k = C_k\,(n_e, T_e)\, n_e n_i \tag{2.9}$$

where n_e and T_e are the electron density and temperature of the plasma, C_k is the emission rate coefficient for the observed transition (emission line) and n_i is the density of the neutral atom or ion being excited. C_k is tabulated in the CHIANTI atomic physics database (Dere et al. 1997) as a function of electron density and temperature for the UV lines of sulfur and oxygen that are observed. The emitted intensity of an electron impact excited line is then

$$I = \int_{-\infty}^{\infty} \rho_k dy = \int_{-\infty}^{\infty} C_k\left(n_e, T_e\right) n_e n_i dy \tag{2.10}$$

where y is the direction along the line of sight.

2.3 Creating the neutral clouds: Sputtering

The material observed in the corona and neutral clouds all originated at Io: Gases are released from volcanic vents, sublimated from frosty regions of the surface, and sputtered (see below) off the surface by incident charged particles. This material either remains in the atmosphere or snows out farther away from the active volcanic centers. In these regions the atmosphere is maintained by vapor pressure equilibrium with the surface. At the atmospheric exobase, some sputtered atoms escape with ballistic trajectories into the exosphere where there are no collisions or other interactions between neutrals. Below I present the flux speed distribution used to characterize the sputtering process.

Sputtering occurs when an ion striking the surface or atmosphere initiates a cascade of collisions which results in the ejection of a neutral (Figure 2.3, and see Johnson (1990)). I use the modified sputtering flux-speed distribution introduced by Smyth and Combi (1988b) to parameterize the speed distribution of sputtered atoms. The single particle speed distribution function is given by:

$$f(v) \propto \frac{1}{\left(v^2 + v_b^2\right)^{\alpha}} \left[1 - \left(\frac{v^2 + v_b^2}{v_M^2}\right)^{1/2}\right] \tag{2.11}$$

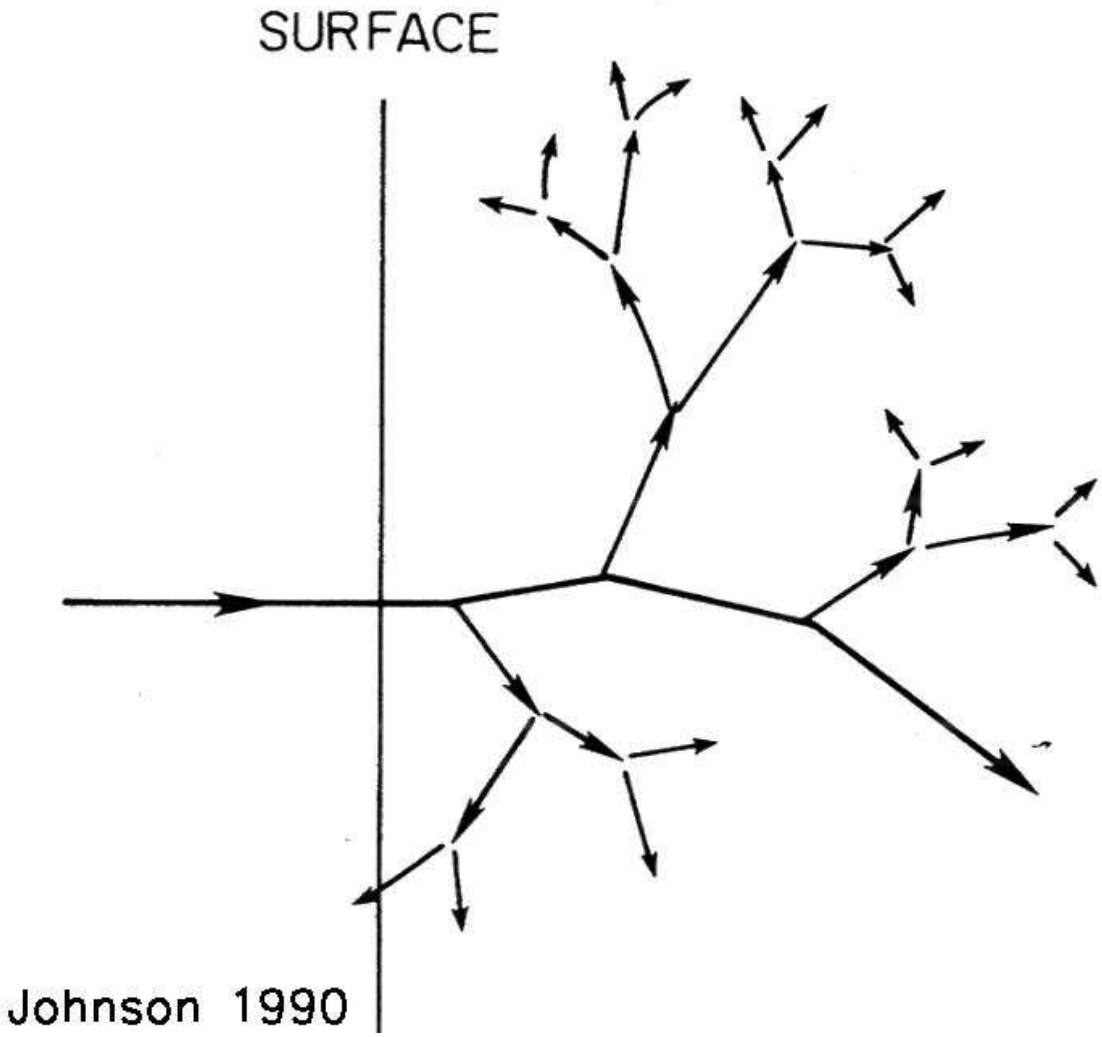

Figure 2.3 Sketch of collisional cascade which results in surface sputtering. Atmospheric sputtering can be represented by a similar sketch with "surface" replaced with "exobase." Figure from Johnson (1990)

where $v_M = \frac{2m_n}{m_{ion}+m_n} v_R$ is the velocity a sputtered atom would have if the atom were ejected from a single completely elastic collision with a torus ion and represents the high speed cutoff of the distribution. m_{ion} and m_n are the masses of the average torus ion and the sputtered neutral, respectively. v_R is the relative speed between the incident ions, which are assumed to be co-rotating with Jupiter's magnetic field, and Io. v_b is related to the energy required to eject a neutral. For pure surface sputtering, the surface binding energy is $mv_b^2/2$. Because sputtering at Io is a mix of surface and atmospheric sputtering, neither of which are likely to be uniform in composition, the average binding energy is not easily determined. Therefore the speed distributions used in this thesis are described in terms of their most probable speed, v_p, which is a non-linear function of v_b: v_b is chosen such that the speed distribution has the desired most probable velocity. The parameter α regulates the high speed behavior of the distribution. Physically it is related to the relative importance of single- and multi-ejection events. Classical sputtering (described by Sieveka and Johnson (1984)) is described by $\alpha = 3$.

The flux distribution for this process is given by

$$\begin{aligned} \phi(v) &\propto v^3 f(v) \\ &\propto \frac{v^3}{\left(v^2+v_b^2\right)^\alpha}\left[1-\left(\frac{v^2+v_b^2}{v_M^2}\right)^{1/2}\right] \end{aligned} \tag{2.12}$$

examples of which are shown in Figure 2.4 for several values of v_p and α. Note that the escape speed from Io' exobase is 2.1 km s^{-1}, so for a low energy sputtering distribution only the high speed tail is important for forming the extended cloud. Panel (a) compares the shapes of sputtering distributions with different values of α. This parameter describes the high speed sputtered material such that the distribution decreases proportional to $v^{3-2\alpha}$ for $v_p < v < v_M$, with a much more rapid drop-off for $v \sim v_M$. The high speed power law drop-off is not affected by the most probable speed as demonstrated in panel (b).

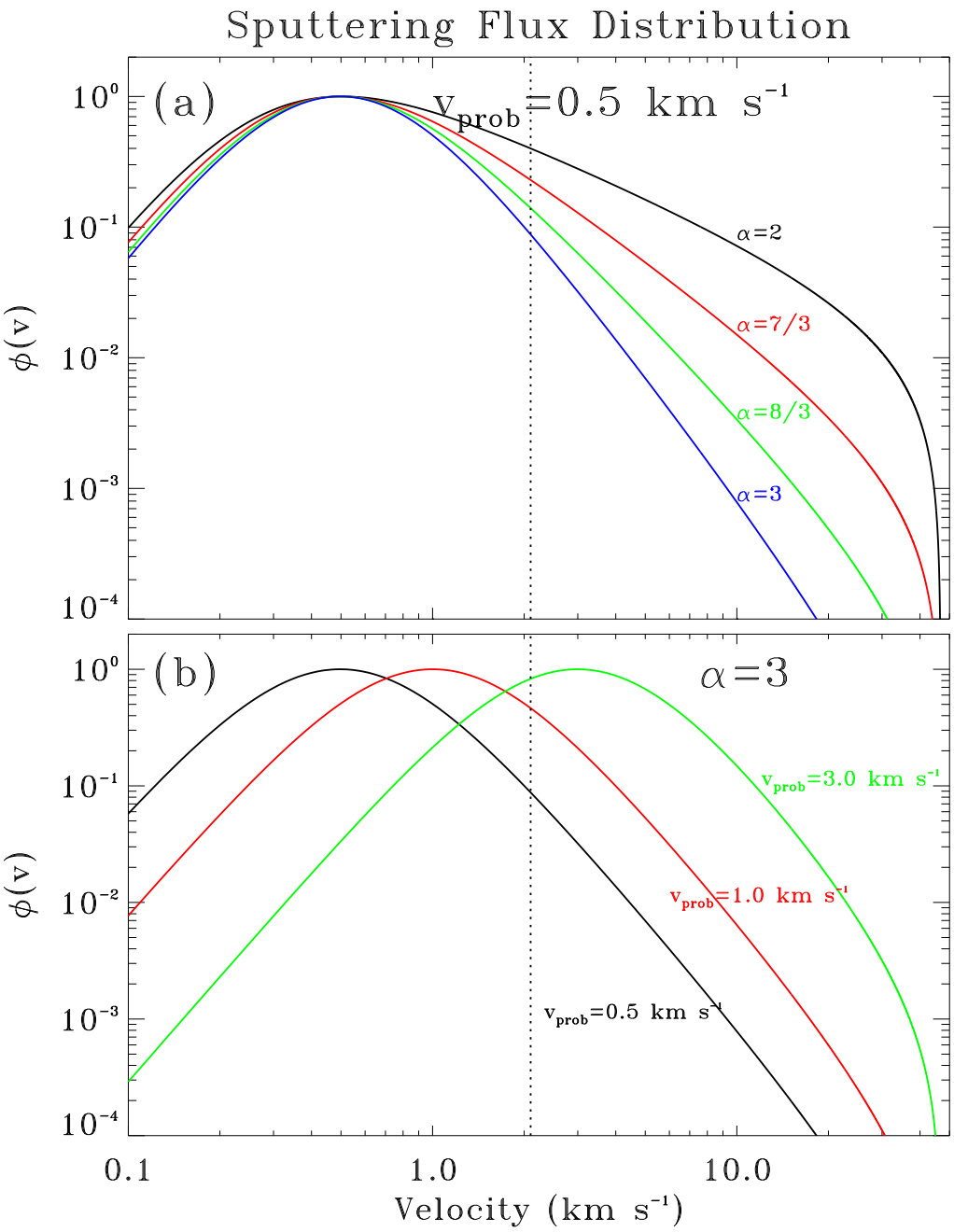

Figure 2.4 Examples of the sputtering flux distribution used as a possible initial flux distribution from Io's exosphere. The normalization is relative to the most probable speed of the distribution. (a) Flux distributions formed by varying α, keeping the most probable speed of the distribution constant at $v_p = 0.5$ km s^{-1}. The dotted line shows the escape velocity from Io's exobase ($v_{esc} = 2.1$ km s^{-1}). (b) Flux distributions keeping α=3 (classical sputtering) and varying the most probable speed.

2.4 Destruction Physics

All the neutral atoms ejected from Io's exobase are eventually lost from the system. In this thesis, two types of loss will be considered: a neutral can hit a large object and be lost to the system or it can be ionized and swept into the plasma torus. Only two objects are considered as sinks for sodium. A neutral can re-impact Io's atmosphere if it is not ejected with sufficient energy to escape Io's gravitational pull. Neutrals can also hit Io if by chance they re-intersect Io's orbit when Io is there. This is a relatively rare occurrence, but it is taken into account as a possibility when calculating particle trajectories. The other physical sink is Jupiter: occasionally a neutral's trajectory takes it too close to Jupiter and is lost from the system.

The dominant sink for neutrals is ionization caused by interaction with the plasma torus. Ionization of the neutral clouds provides the source for the torus, so that the plasma torus and the neutral clouds are intimately related. The lifetime of a neutral ejected from the exobase is

$$\tau = \left(\sum \nu_i\right)^{-1} \tag{2.13}$$

where ν_i are the ionization rates of each individual process. Two ionizing mechanisms are considered: electron impact ionization and charge exchange. The former is most important for sodium; the latter is the dominant oxygen sink. Both processes are important for sulfur. A brief description of the methods for determining the lifetime of neutrals for each mechanism is given below. The photo-ionization rates for oxygen ($\sim$ 38000 hours, Smyth and Marconi (2000)) and sodium ($\sim$ 400 hours, Smyth and Combi (1988b)) are significantly longer than either the electron impact or charge exchange ionization rates and are therefore ignored.

2.4.1 Electron Impact ionization

The rate of neutral ionization due to electron impacts is given by:

$$\nu_{EI} = n_e K\left(T_e\right) \tag{2.14}$$

where n_e and T_e are the electron density and temperature, respectively, at the location of the neutral atoms and $K(T_e)$ is the rate coefficient. The rate coefficient depends on the cross section for ionization which is determined experimentally. Two published measurements of the sodium cross section are shown in Figure 2.5(a). The older measurement (Zapesochnyi and Aleksakhin 1969) is included to provide consistency with previous neutral cloud models (e.g. Smyth and Combi (1988b)). All modeling results in later chapters use the cross section measured by Johnston and Burrow (1995) except where explicitly stated otherwise. This change in atomic data has an effect on the understanding of the neutral cloud due to the fact that the lifetime of sodium at Io is ~ 1.4 times longer than previously thought. Implications for changing the sodium lifetime are considered when discussing model results in Chapters 6 and 7.

The rate coefficient K is a measure of how difficult it is for a given species to be ionized by plasma of a given temperature. I have determined the rate coefficient as a function of electron energy (temperature) using the method of Arnaud and Rothenflug (1985) who empirically parameterize the cross sections shown in Figure 2.5(a) and integrate over a Maxwellian velocity distribution. The rate coefficients for sodium, oxygen, and sulfur are shown in Figure 2.5(b).

Once the rate coefficient is determined, the lifetime of the neutral follows easily from the product of the local electron density and the temperature dependent rate coefficient. Table 2.2 lists typical lifetimes at Io for sodium, oxygen, and sulfur. Since the lifetimes of all species are strongly dependent on the plasma properties, a further analysis of the lifetime will be presented in Chapter 5 when the implementation of the plasma torus is discussed.

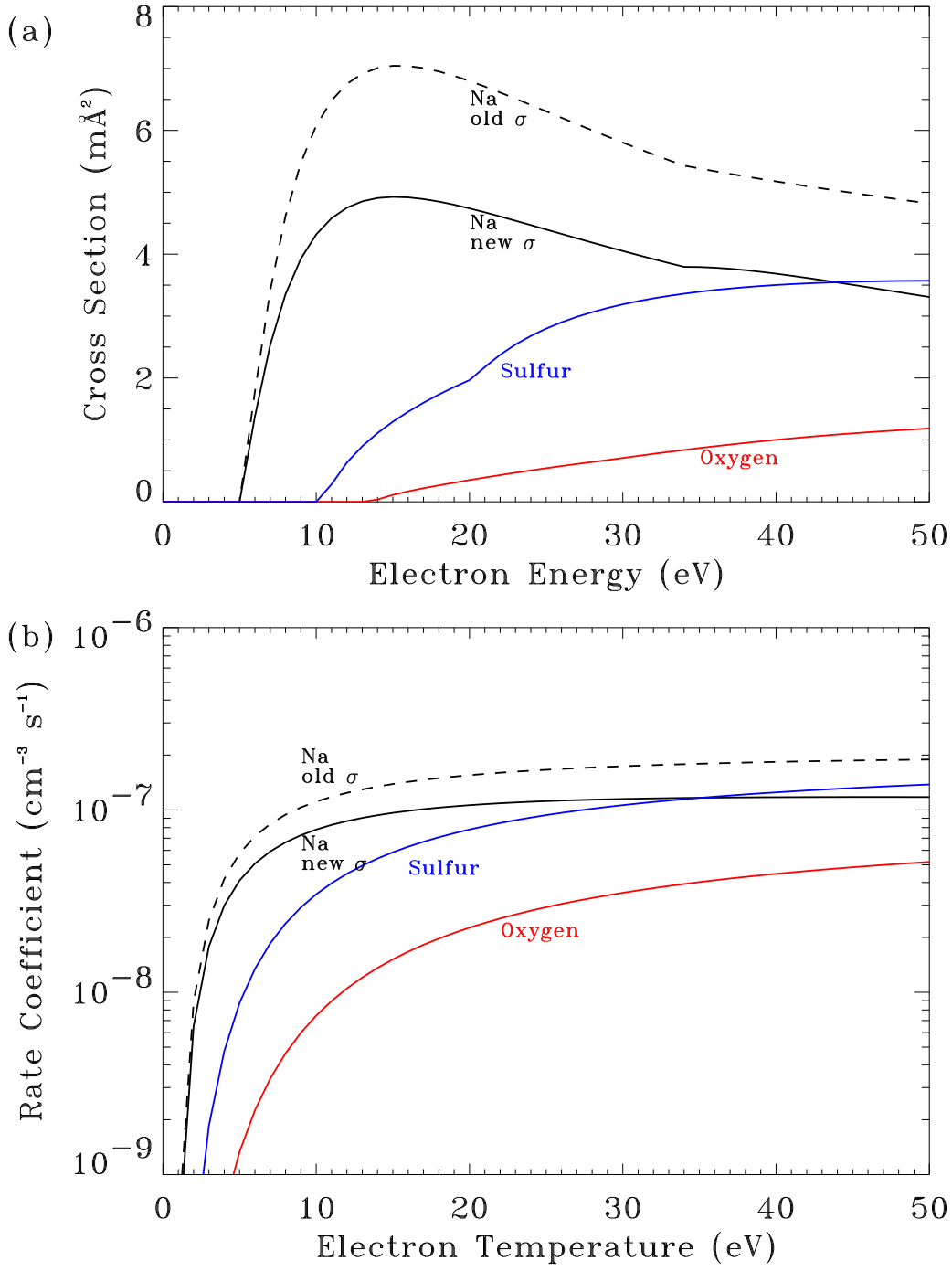

Figure 2.5 (a) Electron impact ionization cross sections. Neutral sodium cross sections determined by Johnston and Burrow (1995) are shown with a solid line. The older measurements of Zapesochnyi and Aleksakhin (1969) are drawn with the broken line. Cross sections for oxygen and sulfur are shown in blue and red, respectively (Arnaud and Rothenflug 1985). (b) Rate coefficients for sodium, oxygen, and sulfur determined from the cross sections in (a).

Species	Electron impact	Charge exchange
Sodium	4 hours	50 hours
Oxygen	150 hours	30 hours
Sulfur	20 hours	30 hours

Table 2.2 Approximate average neutral lifetimes of sodium, oxygen, and sulfur for the processes of electron impact ionization, and charge exchange at Io.

2.4.2 Charge exchange

As seen in Table 2.2, oxygen and sulfur take much longer to be ionized by electron impacts than sodium. For these neutral species, charge exchange with Io torus ions is a significant loss mechanism from the neutral clouds. Charge exchange is a collisional process between two species, at least one of which is ionized, during which the electron clouds of the two species overlap and an electron may be transferred. Loss by charge exchange depends depends on the densities of the different torus species and is therefore affected by both temporal and spatial variations in the plasma torus.

The ionization rate per neutral due to charge exchange, ν_{CX}, is determined by:

$$\nu_{CX} = \sum_i \nu_i = \sum_i \sigma_i v(\mathbf{r}) n_{ion}(\mathbf{r}) \tag{2.15}$$

where the sum is performed over each possible charge exchange reaction. σ_i is the charge exchange cross section for reaction i, and $n_{ion}(\mathbf{r})$ is the density of the torus ion in reaction i at distance $\mathbf{r}$ from Jupiter. $v(\mathbf{r})$ is the relative velocity of ions and neutrals. Torus ions are assumed to be co-rotating rigidly with Jupiter's magnetic field so that:

$$v_{ion} = \Omega r \tag{2.16}$$

with Ω equal to the the angular velocity of Jupiter's magnetic field. The neutral velocity is approximated by the Keplerian velocity appropriate for their distance from Jupiter:

$$v_n = \left(\frac{GM_J}{r}\right)^{(1/2)} \tag{2.17}$$

Therefore, the relative velocity is

$$v(\mathbf{r}) = v_{ion} - v_n = \Omega r - \left(\frac{GM_J}{r}\right)^{(1/2)} \tag{2.18}$$

The important charge exchange reactions for sodium, oxygen, and sulfur are listed in Table 2.3 with their cross sections and rate coefficients at Io's orbit ($k = \sigma v(r = 5.91\,\mathrm{R_J})$).

2.5 Neutral Dynamics

Between their ejection into the Jovian system and their eventual loss, Iogenic neutrals are subjected to the relentless forces of gravity and radiation pressure. The positions of particles are determined by solving the equations of motion defined by:

$$m_n \frac{d^2\mathbf{x_n}}{dt^2} = \sum_i \mathbf{F_i} \tag{2.19}$$

where m_n and $\frac{d^2\mathbf{x}}{dt^2}$ are the mass and acceleration, respectively, of neutral species n, and $\mathbf{F_i}$ are the individual forces of Jupiter's gravity, Io's gravity, and radiation pressure. The following are brief descriptions of these forces as they relate to neutrals in the inner Jovian system.

2.5.1 Gravity

The classical gravitational force is appropriate for the neutrals leaving Io:

$$\mathbf{F} = -G\frac{M_p m_n}{r_p^2}\hat{r} \tag{2.20}$$

where G is the universal Gravitational constant, M_p is the mass of the object exerting the force (i.e., Jupiter and Io), r_p is the distance from the neutral to that object, and m_n is the mass of the neutral. The acceleration caused by the gravitational force is what is actually important, so:

$$\mathbf{a} = -G\frac{M_p}{r_p^2}\hat{r} \tag{2.21}$$

which is independent of the mass of the neutral being considered. This is important because it means that the neutrals considered in this thesis behave identically when injected into the system when only gravity is considered. Differences in cloud morphologies are due to factors other than their dynamical behaviors when added to the Jovian system.

Reaction	σ ($\mathbf{\AA^{-2}}$)	**k** ($\mathbf{10^{-9}\ cm^3 s^{-1}}$)
$O + O^+ \rightarrow O^+ + O$	22	13
$O + O^{++} \rightarrow O^{++} + O$	9	0.5
$O + O^{++} \rightarrow O^+ + O^+$	0.9	5
$O + S^+ \rightarrow O^+ + S$	0.1	0.06
$O + S^{++} \rightarrow O^+ + S^+$	3.8	2.2
$O + S^{+++} \rightarrow O^+ + S^{++}$	32	18
$S + O^+ \rightarrow S^+ + O$	5	3
$S + O^{++} \rightarrow S^{++} + O$	39	22
$S + S^+ \rightarrow S^+ + S$	40	23
$S + S^{++} \rightarrow S^+ + S^+$	0.5	0.3
$S + S^{++} \rightarrow S^{++} + S$	13	7.4
$S + S^{+++} \rightarrow S^+ + S^{++}$	22	12
$Na + O^+ \rightarrow Na^+ + O$	0	0
$Na + O^{++} \rightarrow Na^+ + O^+$	~ 30	17
$Na + S^+ \rightarrow Na^+ + S$	0	0
$Na + S^{++} \rightarrow Na^+ + S^+$	~ 30	17

Table 2.3 Summary of the major charge exchange reactions between neutral oxygen and sulfur atoms and the major torus ions. Cross sections are compiled from McGrath and Johnson (1989) The rate coefficients are calculated at the distance of Io's orbit.

2.5.2 Radiation Pressure

More than just a perturbation, radiation pressure can have a real effect on the dynamics of neutrals ejected from Io. Because the resonant transition of sodium is near the peak of the solar black body continuum, radiation pressure is most important for understanding the evolution of sodium. Oxygen and sulfur have resonant transitions at FUV wavelengths (1304 Å and 1299 Å, respectively) where the solar continuum is very weak, and therefore radiation pressure is not a factor affecting these species.

Radiation pressure is a force exerted on a cloud of atoms due to the absorption and emission of photons by the gas. The isotropic scattering of photons that causes the sodium cloud to be visible also results in a force equal to the rate of change in the net momentum of the absorbed photons:

$$\mathbf{F} = \frac{d\mathbf{p}}{dt} \tag{2.22}$$

Since the photons are all initially incident from the direction of the sun, the magnitude of the momentum of a single photon is

$$p_{phot} = \frac{h}{\lambda} \tag{2.23}$$

where h is Planck's Constant, c is the speed of light, and λ is the wavelength of the absorbed photon. Therefore the net change in momentum of the neutral is equal to the momentum of the incident absorbed photons, i.e.

$$\frac{d\mathbf{p}}{dt} = g \times \mathbf{p_{phot}} \tag{2.24}$$

where g is the rate of photon absorption by a neutral atom given by Equation 2.7.

The acceleration due to the resonant scattering of photons therefore:

$$\begin{aligned} a_{rad} &= \frac{F_{rad}}{m_{Na}} \\ &= \sum_{l=D_1,D_2} \frac{g_l \cdot p_{phot}}{m_{Na}} \\ &= \sum_{l=D_1,D_2} \frac{1}{m_{Na}} \cdot \left[\gamma_l \cdot \pi F_\odot \cdot \frac{\lambda^2}{c}\right] \cdot \left[\frac{\pi e^2}{m_e c} \cdot f_l\right] \left[\frac{h}{\lambda}\right] \\ &= \left[\frac{\pi F_\odot \lambda h}{c m_{Na}}\right] \left[\frac{\pi e^2}{m_e c}\right] [\gamma_1 f_1 + \gamma_2 f_2] \end{aligned} \tag{2.25}$$

Using the values appropriate for sodium, the radiation pressure acceleration is a function only of γ for each line, which in turn is a function of the radial velocity of Io relative to the sun. The radiation pressure term in the equations of motion is therefore:

$$a_{rad} = 0.580\,(\gamma_1 + 2\gamma_2)\ cm\,s^{-2} \tag{2.26}$$

In Io's corona, at 3 R_{Io}, the acceleration due to Io's gravity on a neutral atom is 20 cm s^{-2}, the centripetal acceleration toward Jupiter of a sodium atom in orbit around Jupiter at Io's orbit is 70 cm s^{-2}, and the acceleration due to radiation pressure of a sodium atom at western elongation, where the radial velocity is maximized, is 1 cm s^{-2}. Although the radiation pressure term is large enough to perturb the orbits of sodium atoms, it is too small to have any observable consequences. The effect of radiation pressure is discussed in more detail in Chapter 5.

2.6 Summary

Each step in the lives of the atoms which make up the neutral clouds can is dominated by no more than two process. Their birth into the system is represented by ejection from the exobase into the corona. This is dominated by the process of sputtering of Io's atmosphere by the plasma torus. The behavior of the neutrals once they escape from the near-surface atmosphere is governed by the competing effects of Io's and Jupiter's gravitational attraction. In the corona, Io's gravity is the dominant

force; farther out, Jupiter wins out. Atoms are lost from the system by either electron impact ionization or charge exchange with torus ions. The former process dominates the sodium loss from the neutral clouds, although charge exchange near Io's exobase has important observational consequences. Charge exchange is the most important loss mechanism for oxygen. Sulfur is lost through both electron impact ionization and charge exchange.

In the following chapters, different aspects of Io's corona and neutral clouds are described and modeled. All of the features which are discussed result from different combinations of the physical processes discussed here.